N 62 70950

NASA TN D-376

NASA TN D-376

7N-05
193972
P-23

TECHNICAL NOTE

D-376

HIGH-TIP-SPEED STATIC-THRUST TESTS OF A ROTOR HAVING NACA $63_{(215)}$A018 AIRFOIL SECTIONS WITH AND WITHOUT VORTEX GENERATORS INSTALLED

By James P. Shivers

Langley Research Center
Langley Field, Va.

NATIONAL AERONAUTICS AND SPACE ADMINISTRATION

WASHINGTON May 1960

NATIONAL AERONAUTICS AND SPACE ADMINISTRATION

TECHNICAL NOTE D-376

HIGH-TIP-SPEED STATIC-THRUST TESTS OF A ROTOR HAVING NACA $63_{(215)}$A018 AIRFOIL SECTIONS WITH AND WITHOUT VORTEX GENERATORS INSTALLED

By James P. Shivers

L
3
1
1

SUMMARY

An investigation has been made on a rotor having NACA $63_{(215)}$A018 airfoil sections over approximately the outer 0.5 radius to determine the maximum mean lift coefficients at low tip Mach numbers and the compressibility effects at high tip Mach numbers. The maximum mean lift coefficient obtained for this rotor was 1.06. At a tip Mach number of 0.71, the rotor encountered compressibility drag losses at a rotor-blade mean lift coefficient of about 0.40. The pitching moments of the rotor blades were small, and the nosedown pitching-moment break was delayed beyond the point where the profile power started to increase.

The use of vortex generators to alleviate rotor-blade stall produced significant gains in rotor-blade mean lift coefficients, although with some penalty in profile torque at low lift coefficients.

INTRODUCTION

One means of reducing compressibility losses on a helicopter rotor is to employ a reasonably small thickness-chord ratio of the blade. This solution may not always be possible. For example, if a pressure-jet system were employed on a helicopter, the use of an airfoil of conventional thickness-chord ratio would require that small internal ducts be used in the blade, and these small ducts may, in turn, lead to relatively large internal losses. Thus, for pressure-jet rotor systems, it may be necessary to accept greater external compressibility losses in order to maintain reasonably efficient internal flow.

In order to select an airfoil section for a pressure-jet rotor system, it is necessary to know the performance that will be obtained by using relatively thick airfoil sections in the rotor. The present paper gives the performance of a rotor having NACA $63_{(215)}$A018 airfoil sections. This test is a continuation of a general research program (refs. 1 to 6) investigating performance characteristics of similar rotors for which airfoil section is the primary variable. Although the data are obtained for the hovering condition, the onset and rate of growth of stall and compressibility effects can be analyzed qualitatively to aid in the selection of airfoil sections for high-speed rotors in forward flight.

The hovering performance of the rotor is presented for a tip Mach L
number range from 0.27 to 0.76 and a corresponding blade tip Reynolds 3
number range from 1.67×10^6 to 4.59×10^6. The rotor was tested at 1
disk loadings as high as 7.0 pounds per square foot. The maximum lift 1
of the rotor at low tip Mach numbers and the drag-divergence characteristics at higher Mach numbers are discussed and compared with unpublished two-dimensional NACA 64_3-018 airfoil data previously obtained in the Langley low-turbulence pressure tunnel.

The performance characteristics of thick airfoil sections may be seriously limited by stall starting at the trailing edges of the airfoils. In order to extend the usable performance of the rotor to higher lift coefficients, vortex generators were installed on the blades for a portion of the tests. The hovering performance of the rotor with the vortex generator installed is presented and compared with the performance of the smooth-blade rotor.

SYMBOLS

b number of blades

C_m rotor-blade pitching-moment coefficient, $\dfrac{M_Y}{R\frac{\rho}{2}(\Omega R)^2 c_e{}^2}$

C_Q rotor torque coefficient, $\dfrac{Q}{\pi R^2 \rho (\Omega R)^2 R}$

$C_{Q,o}$ rotor profile-drag torque coefficient, $\dfrac{Q_o}{\pi R^2 \rho (\Omega R)^2 R}$

C_T rotor thrust coefficient, $\dfrac{T}{\pi R^2 \rho (\Omega R)^2}$

c	blade chord at radius r, ft
c_d	airfoil-section drag coefficient
$c_{d,o}$	airfoil-section profile drag coefficient
c_e	equivalent blade chord, $\dfrac{\int_0^R cr^2 dr}{\int_0^R r^2 dr}$, ft
c_l	rotor-blade lift coefficient
$\overline{c_l}$	mean rotor-blade lift coefficient, $6C_T/\sigma$
c_t	blade chord at tip
M	rotor-blade Mach number
M_t	rotor-blade-tip Mach number
M_Y	rotor-blade pitching moment, lb-ft
$N_{Re,t}$	Reynolds number at blade tip, $\rho\Omega Rc_t/\mu$
Q	rotor torque, lb-ft
Q_o	rotor profile-drag torque, lb-ft
R	rotor-blade radius, ft
r	radial distance to a blade element, ft
T	rotor thrust, lb
α_r	blade section angle of attack, deg or radians as specified
$\alpha_{r,t}$	blade-section-tip angle of attack, deg or radians as specified
θ	blade-section pitch angle measured from line of zero lift, deg
μ	coefficient of viscosity, slugs/ft-sec

ρ mass density of air, slugs/cu ft

σ rotor solidity, $bc_e/\pi R$

Ω rotor angular velocity, radians/sec

APPARATUS AND TEST METHODS

Rotor Blades

L311

A fully articulated, two-blade rotor was used for this investigation. The flapping hinge was located on the center of rotation and the drag hinge was located 12 inches outboard of the center line.

A sketch of the rotor blade with pertinent dimensions is shown in figure 1. The rotor solidity was 0.033, and the radius from the center line of rotation was 18.84 feet. The blades were built of metal with 5.5° of linear washout. Laminated balsa wood covered with fiber glass was added to the blade of reference 1 and contoured so as to maintain an NACA $63_{(215)}$A018 airfoil section over approximately the outer half of the blades. Since the outer 50 percent of the rotor span is responsible for about 75 percent of the rotor thrust and torque, it is believed that the rotor can be considered essentially as a complete rotor having NACA $63_{(215)}$A018 airfoil sections. The surfaces of the airfoils were smooth and fair over the entire chord of the glove.

Test Methods and Accuracy

The rotor was tested on the Langley helicopter test tower. The height of the rotor head above ground level (42 feet) is such that ground effect on the rotor should be negligible. The test procedure was the same as that of reference 1. The blades were tested over a tip Mach number range from 0.27 to 0.76. The tip Mach number of 0.76 was the limiting Mach number due to structural limitations of the rotor blades.

In order to study the flow for conditions near stall, tufts were mounted on the rotor blade in the same manner as that described in reference 1. A high-speed (128 frames per sec) motion-picture camera was mounted on the rotor head to record the tuft motion during the tests at low tip speeds and high pitch angles.

The estimated accuracies of the basic quantities measured during the tests are similar to those of reference 1 and the plotted results are believed to be within ±3 percent.

RESULTS AND DISCUSSION

Results Obtained for Plain Rotor

The rotor thrust, torque, and figure of merit measured over the range of tip Mach numbers are presented in figures 2 to 4. A maximum value of mean lift coefficient $\overline{c_l}$ of 1.06 was obtained for this rotor (fig. 3). This value compares with $\overline{c_l}_{,max} = 1.15$ measured for rotor blades having NACA 63_2-015 airfoil sections. (See ref. 3.) At $M_t = 0.71$, $\overline{c_l}$ reached a value of about 0.40 before drag divergence. Drag divergence was exceeded at zero thrust for a tip Mach number of 0.75. (See fig. 2.)

The rotor efficiency of the present test is similar to that obtained for the rotor of reference 1 for values of $\overline{c_l}$ less than 0.80. Adverse effects of stall above $\overline{c_l} = 0.80$ caused the rotor efficiency to decrease quite rapidly. (See fig. 3.)

Calculated values of the rotor induced torque coefficient were used to determine the measured profile torque coefficients. The measured profile torque coefficient was referenced to the profile torque coefficient calculated with the assumption of no compressibility or stall effects. This ratio is presented in terms of the calculated blade-tip angle of attack and rotor mean lift coefficient in figures 5 and 6, respectively. The profile drag at low tip speeds starts to increase at a tip angle of attack of the order of 6.5° to 7.5°. The early drag divergence at this speed is believed to be caused by stall. The suspected stall is substantiated from the motion pictures showing the tufts mounted on the blade. The stall was observed to occur first at the trailing edge near the midspan and then spread forward and outward as the tip angle of attack was increased. A similar stall condition was observed on the thick airfoils of reference 7. Drag divergence at zero rotor-blade-tip angle of attack occurs between tip Mach numbers of 0.71 and 0.75; this value is slightly lower than that observed for the rotor blade having NACA 0015 airfoil tip sections (ref. 1).

A comparison of the rotor-blade-tip Mach numbers and angles of attack at which drag divergence occurs with those indicated by unpublished two-dimensional NACA 64_3-018 airfoil data (previously obtained in the Langley low-turbulence pressure tunnel) indicates large variations in Mach numbers as divergence occurs with increasing angle of attack (fig. 7). It is believed that the large measured reduction in divergence Mach number at the higher angles of attack is caused by the rotor-blade stall as observed in the motion pictures made of the tufts.

The measured rotor-blade pitching moments (fig. 8) include both mass and aerodynamic moments. The resultant moments are shown to be small and slightly noseup over most of the thrust-coefficient range. It is believed that the shape of the curves is more significant than the actual magnitudes. The nosedown pitching-moment break is delayed beyond the point where profile torque starts to increase.

Tests With Vortex Generators Installed

The rotor performance (fig. 2) shows a rapid increase in rotor- L
blade torque coefficient with a gradual increase in thrust coefficient 3
for values of thrust coefficient over 0.0044. The separated flow, as 1
observed in the high-speed motion pictures, causes the profile torque 1
to increase. Vortex generators were employed as a means of controlling the flow separation over the rearward section of the rotor blade. The vortex generators, as seen in sketch in figure 9, were uniform, were airfoil shaped, and were mounted with their leading edges placed at about the 46-percent blade chord. They were mounted in pairs at 16° angle of attack with respect to a plane perpendicular to the blade span. The trailing edges of the airfoils in each pair were spaced 0.24 inch apart. The height of the airfoils was initially 0.30 inch but after preliminary tests the height was reduced to 0.15 inch. The chord was 0.30 inch, and the gap between pairs of airfoils was 0.20 inch. The generators were installed over the entire length of the blade section having NACA $63_{(215)}$A018 airfoil sections.

The vortex generators, as initially installed, were 0.30 inch high. A few runs with these generators installed indicated that the profile torque was increased prohibitively, so the height was reduced to 0.15 inch. All data presented herein were obtained with the short vortex generators.

No systematic tests were made in order to arrive at an optimum vortex-generator configuration. It is conceivable that suitable changes in height, chordwise location, spanwise spacing, and angle of attack might result in a vortex-generator installation which would have essentially the same effects on lift coefficient but which would produce smaller drag than the present installation.

Performance Measurements

In comparing the hovering performance for the rotor with and without vortex generators (fig. 10), it can be seen that in the low thrust-coefficient range the profile torque coefficient is higher for the blades with the generators. Thus, there is some penalty in power in this particular range. Above $C_T = 0.0048$, however, the installation of generators permitted the blades to reach higher angles of attack before stall reappeared, thereby giving substantial gains in thrust coefficient.

An alternate way of showing the gains in $\overline{c_l}$ is given in figure 11 where the data are referenced to the blade without generators. A study of the motion pictures of the tuft pattern on the rotor without vortex generators indicated that portions of the blade trailing edge were stalled at the higher pitch angles. With the vortex generators installed, the rotor blade had much less stalled area for a given pitch angle. For portions of the azimuth, some stall was indicated at the higher blade pitch angles; this stall was due to small flapping angles caused by a low wind condition. Thus, the gains in rotor-blade mean lift coefficients are obtained by a reduction in stalled area in the higher rotor-blade pitch range.

Rotor Efficiency

The efficiency of the rotor with vortex generators (fig. 12) is less than that of the blade without generators for values of $\overline{c_l}$ below 0.9. This difference is a result of the added profile torque caused by the installation of the vortex generators. Above $\overline{c_l} = 0.9$, however, the efficiency of the rotor with the generators is substantially greater than the efficiency of the one without generators. It is believed that the reduction in flow separation over the rearward portion of the rotor blade yields the improved efficiency.

It is possible that the decrease in rotor efficiency in the low thrust range, as a result of the installation of vortex generators, would be less for a rotor blade of practical construction tested under the same conditions since the production rotor blades would probably have a higher zero-lift profile drag because of manufacturing tolerances than do the smooth rotor blades used in the present investigation. If so, the same absolute increase in torque due to the presence of the vortex generators would represent an appreciably smaller percentage of the total profile torque requirement.

SUMMARY OF RESULTS

A rotor blade having NACA $63_{(215)}$A018 airfoil sections over approximately the outer 0.5 radius has been tested with and without vortex generators throughout a tip Mach number range from 0.27 to 0.76. The results of this investigation were as follows:

1. The maximum rotor-blade mean lift coefficient obtained was 1.06. This value may be compared with a value of 1.15 measured previously on a rotor having NACA 63_2-015 airfoil sections.

2. At a tip Mach number of 0.71, the rotor-blade mean lift coefficient reached a value of about 0.40 before drag divergence. At a tip Mach number of 0.75, an increase in profile-drag torque due to compressibility effects was indicated even at zero thrust.

L
3
1
1

3. The pitching moments were small and were slightly noseup over most of the thrust-coefficient range. The nosedown pitching-moment break was delayed beyond the point where profile torque started to increase.

4. The figures of merit obtained for the present rotor without vortex generators were close to those obtained on the rotor blades having NACA 0015 tip airfoil sections up to a rotor-blade mean lift coefficient of about 0.80. At higher thrust the adverse effects of stall reduced the efficiency quite rapidly.

5. Motion pictures of tufts mounted on the rotor blade indicated that stalling was initiated in the region of the trailing edge and gradually spread forward. The same trend was shown in previous two-dimensional tests of airfoils with similar thickness ratios.

6. The use of vortex generators to alleviate rotor-blade stall produced significant gains in maximum rotor-blade mean lift coefficients with some penalty in profile torque at low lift coefficients.

Langley Research Center,
National Aeronautics and Space Administration,
Langley Field, Va., February 4, 1960.

REFERENCES

1. Shivers, James P., and Carpenter, Paul J.: Effects of Compressibility on Rotor Hovering Performance and Synthesized Blade-Section Characteristics Derived From Measured Rotor Performance of Blades Having NACA 0015 Airfoil Tip Sections. NACA TN 4356, 1958.

2. Carpenter, Paul J.: Effects of Compressibility on the Performance of Two Full-Scale Helicopter Rotors. NACA Rep. 1078, 1952. (Supersedes NACA TN 2277.)

3. Shivers, James P., and Carpenter, Paul J.: Experimental Investigation on the Langley Helicopter Test Tower of Compressibility Effects on a Rotor Having NACA 63_2-015 Airfoil Sections. NACA TN 3850, 1956.

4. Powell, Robert D., Jr., and Carpenter, Paul J.: Low Tip Mach Number Stall Characteristics and High Tip Mach Number Compressibility Effects on a Helicopter Rotor Having an NACA 0009 Tip Airfoil Section. NACA TN 4355, 1958.

5. Powell, Robert D., Jr.: Compressibility Effects on a Hovering Helicopter Rotor Having an NACA 0018 Root Airfoil Tapering to an NACA 0012 Tip Airfoil. NACA RM L57F26, 1957.

6. Carpenter, Paul J.: Lift and Profile-Drag Characteristics of an NACA 0012 Airfoil Section as Derived From Measured Helicopter-Rotor Hovering Performance. NACA TN 4357, 1958.

7. McCullough, George B., and Gault, Donald E.: Examples of Three Representative Types of Airfoil-Section Stall at Low Speed. NACA TN 2502, 1951.

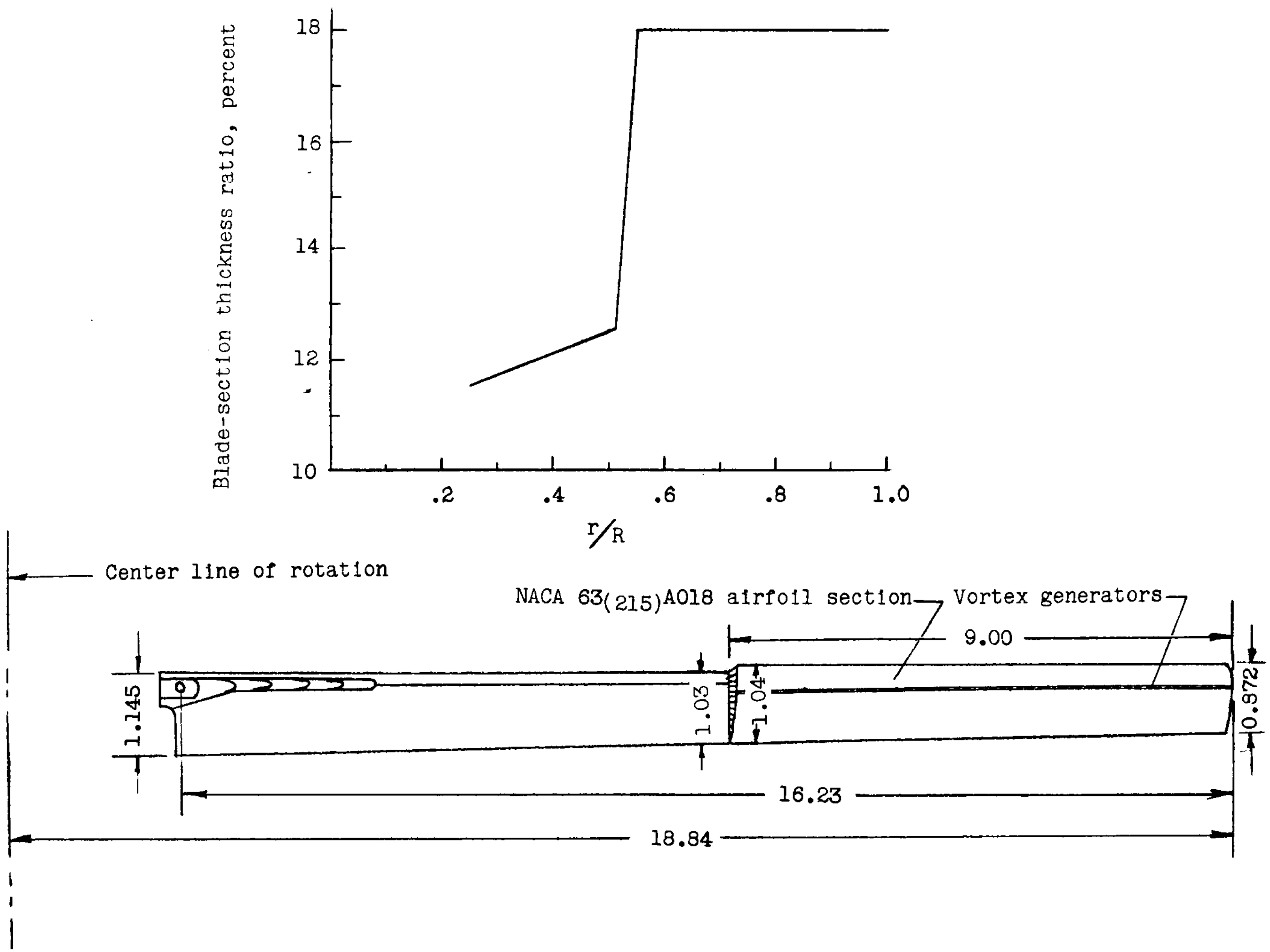

Figure 1.- Sketch of rotor blade having NACA $63_{(215)}$A018 airfoil section on the outer 9 feet of radius. Rotor blade washout is 5.5°. Equivalent blade chord is 0.966 foot; σ = 0.033. All dimensions are in feet.

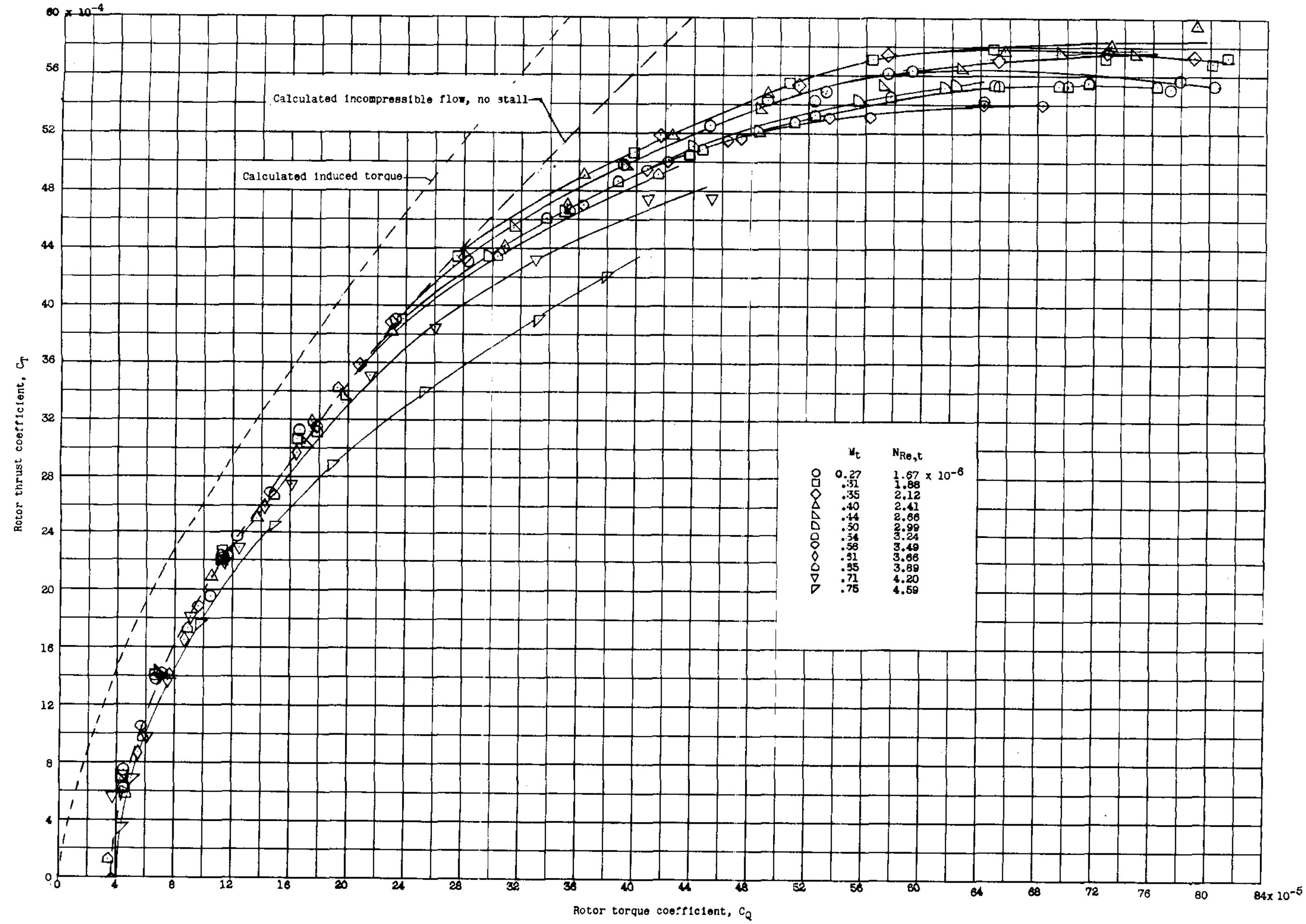

Figure 2.- Hovering performance of rotor blades having NACA $63_{(215)}$A018 airfoil tip sections. Calculated curve based on $c_{d,o} = 0.0087 - 0.0216\alpha_r + 0.400\alpha_r^2$ and $c_l = 5.73\alpha_r$; $\sigma = 0.033$.

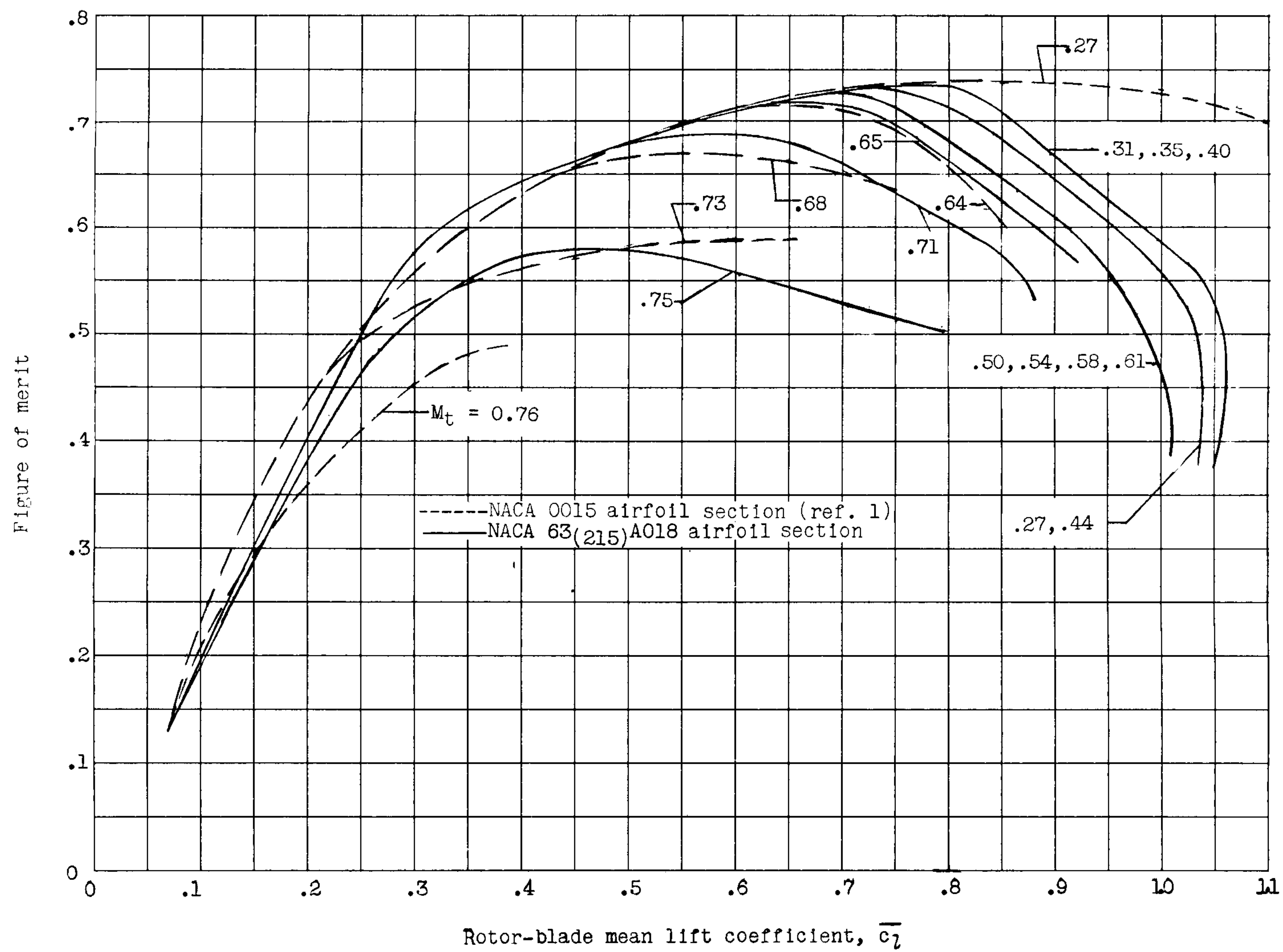

Figure 3.- Effect of tip Mach number on rotor figure of merit. Results are compared with results of tests on rotor having NACA 0015 airfoil sections (ref. 1).

L-311

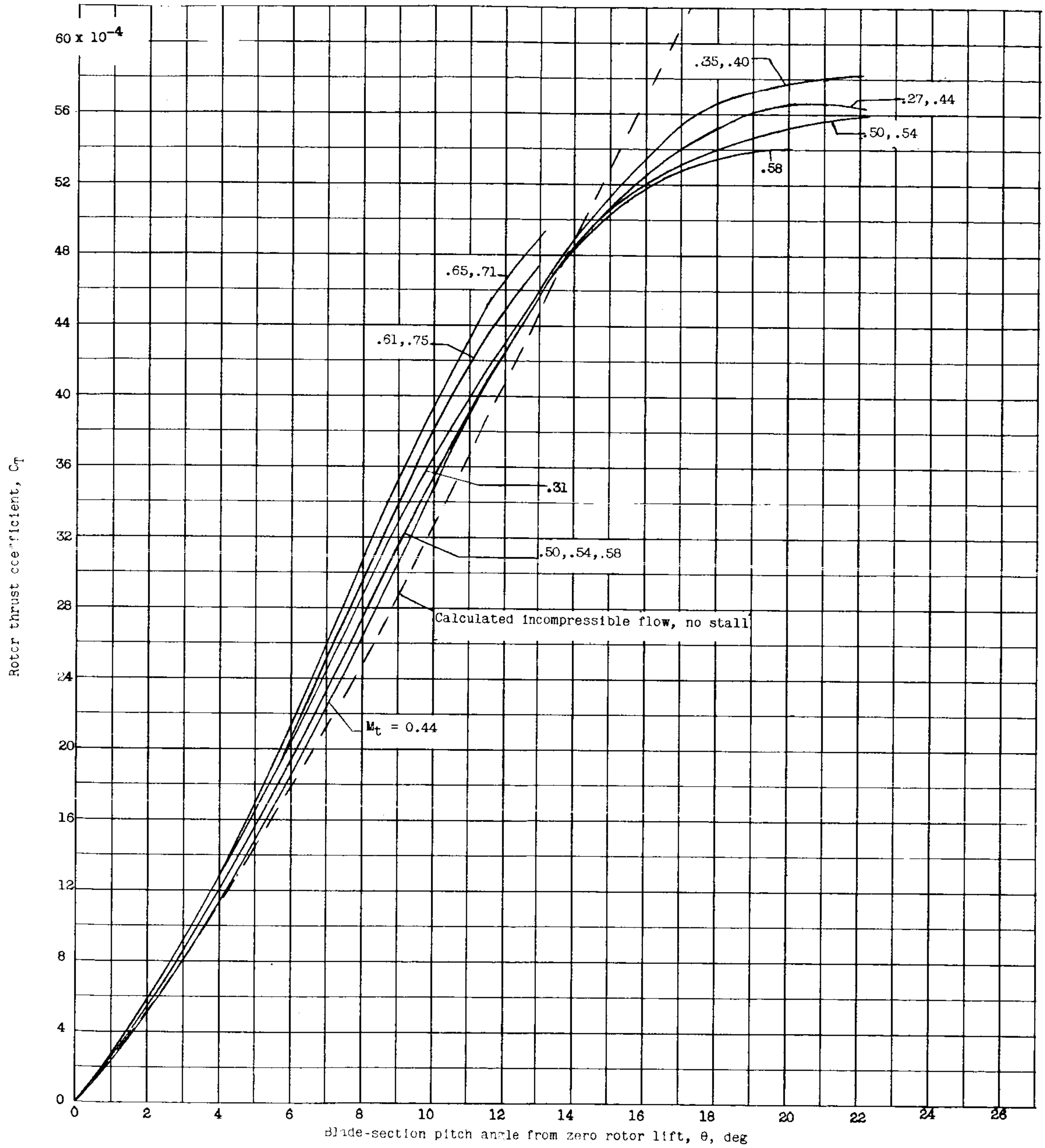

Figure 4.- Effect of tip Mach number on rotor thrust coefficient.

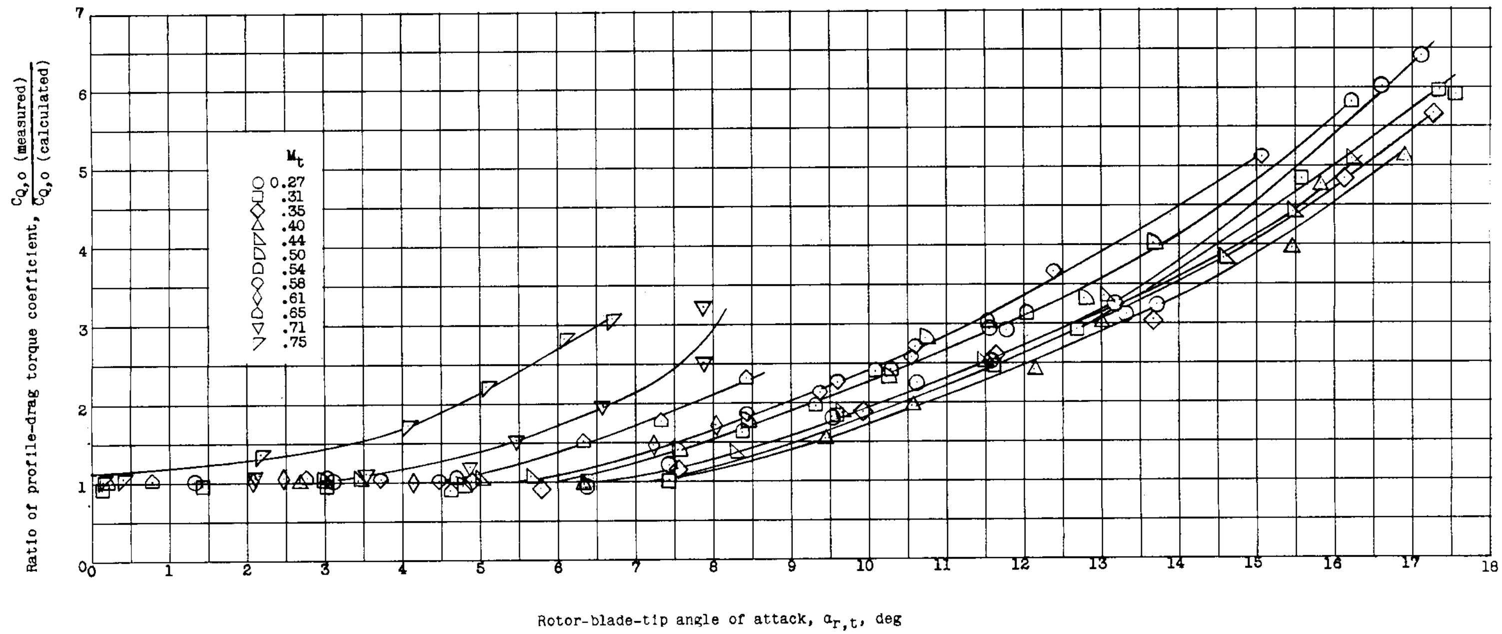

Figure 5.- Effect of tip angle of attack and Mach number on ratio of profile-drag torque coefficient.

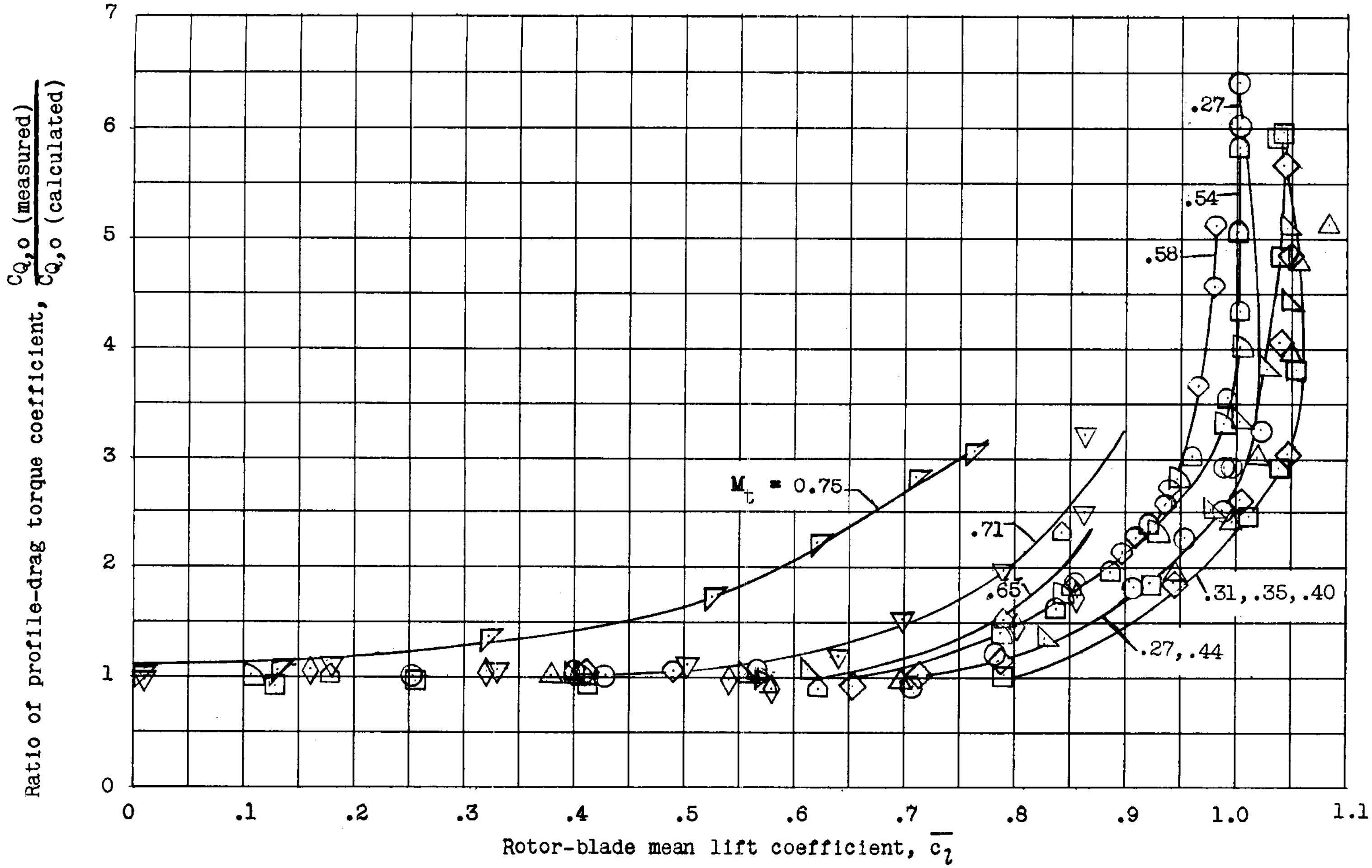

Figure 6.- Effect of rotor-blade mean lift coefficient and Mach number on ratio of profile-drag torque coefficient.

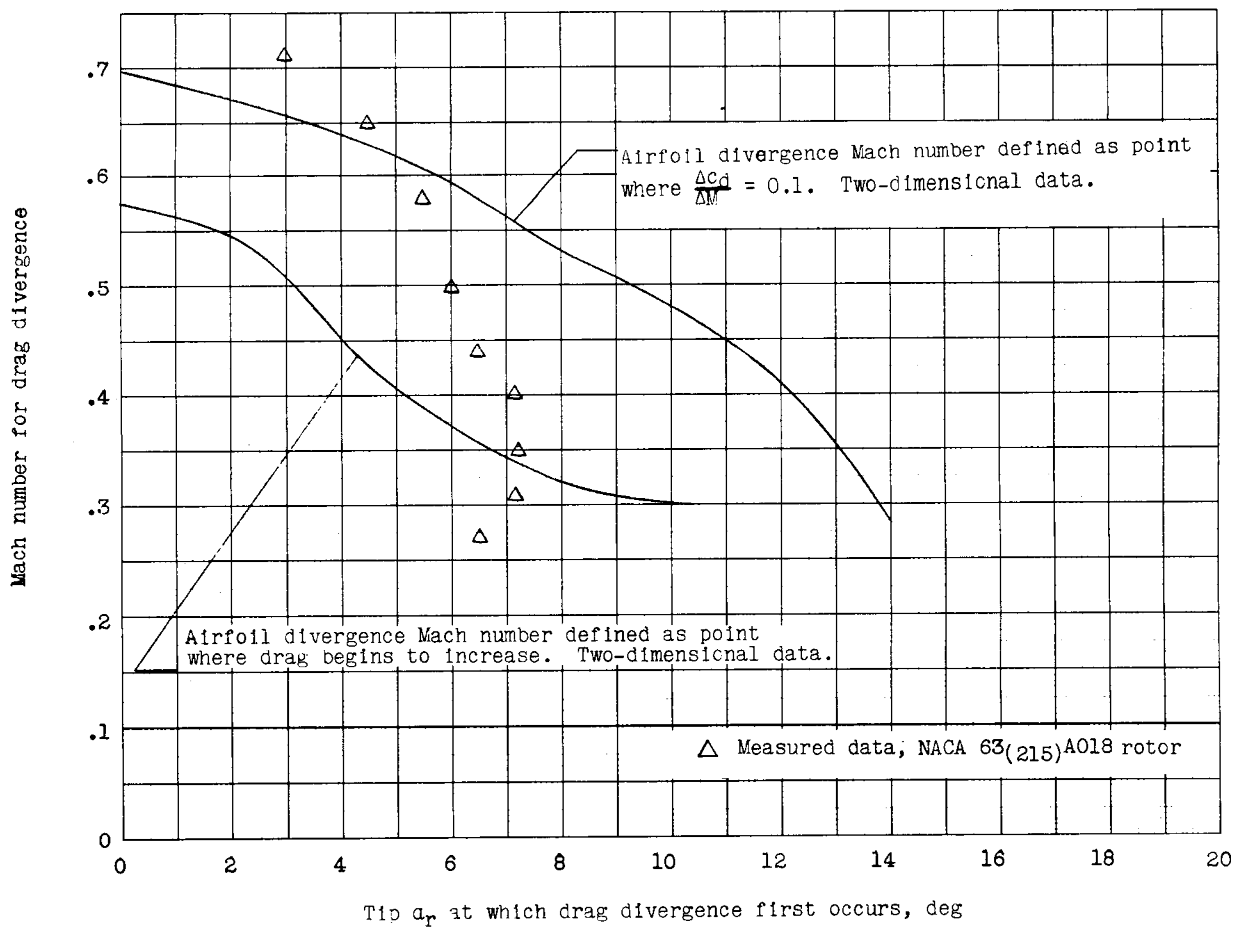

Figure 7.- Comparison of unpublished two-dimensional airfoil drag-divergence data (previously obtained on NACA 64_3-018 airfoils in the Langley low-turbulence pressure tunnel) with rotor experimental data. Test point symbols represent values of M_t and $\alpha_{r,t}$ at which experimental data from rotor blade separate from curve calculated by using airfoil drag polar $c_{d,o} = 0.0087 - 0.0216\alpha_r + 0.400\alpha_r^2$.

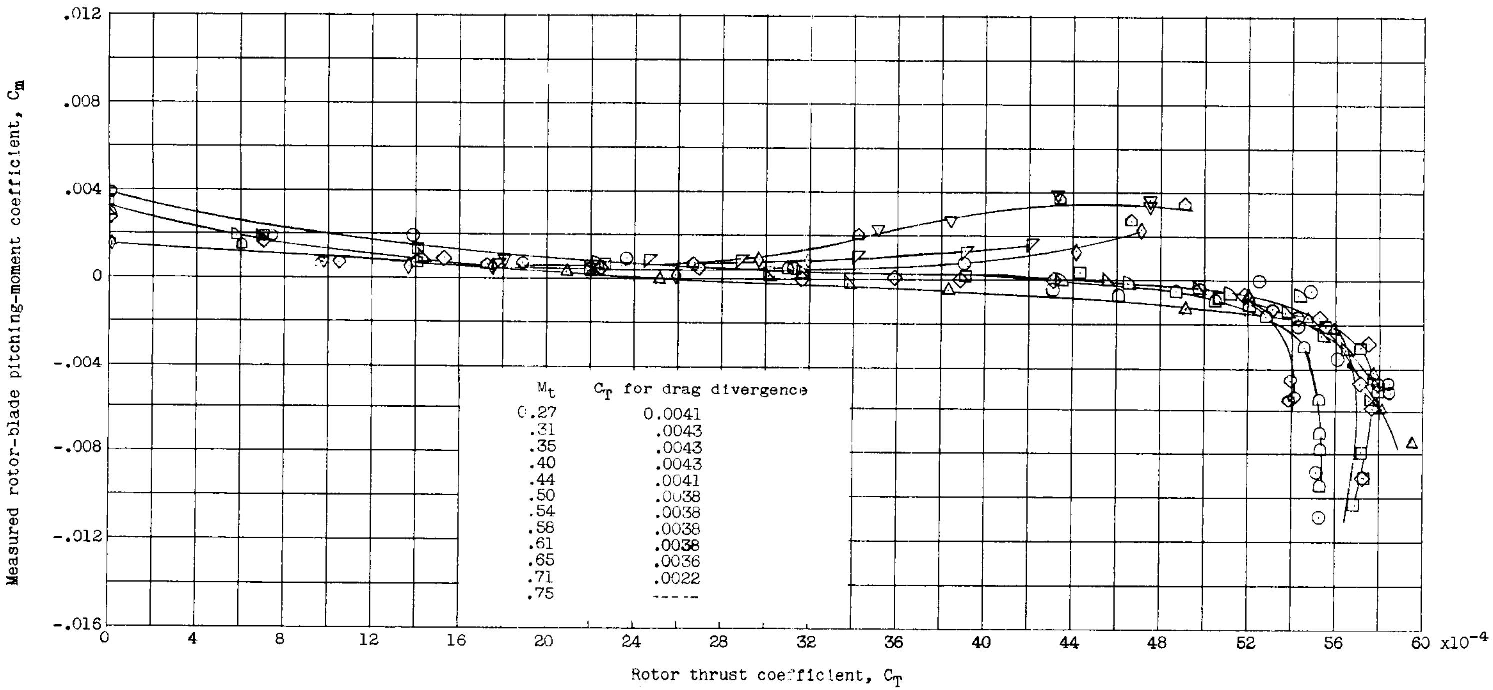

Figure 8.- Effect of tip Mach number on the rotor-blade pitching moment.

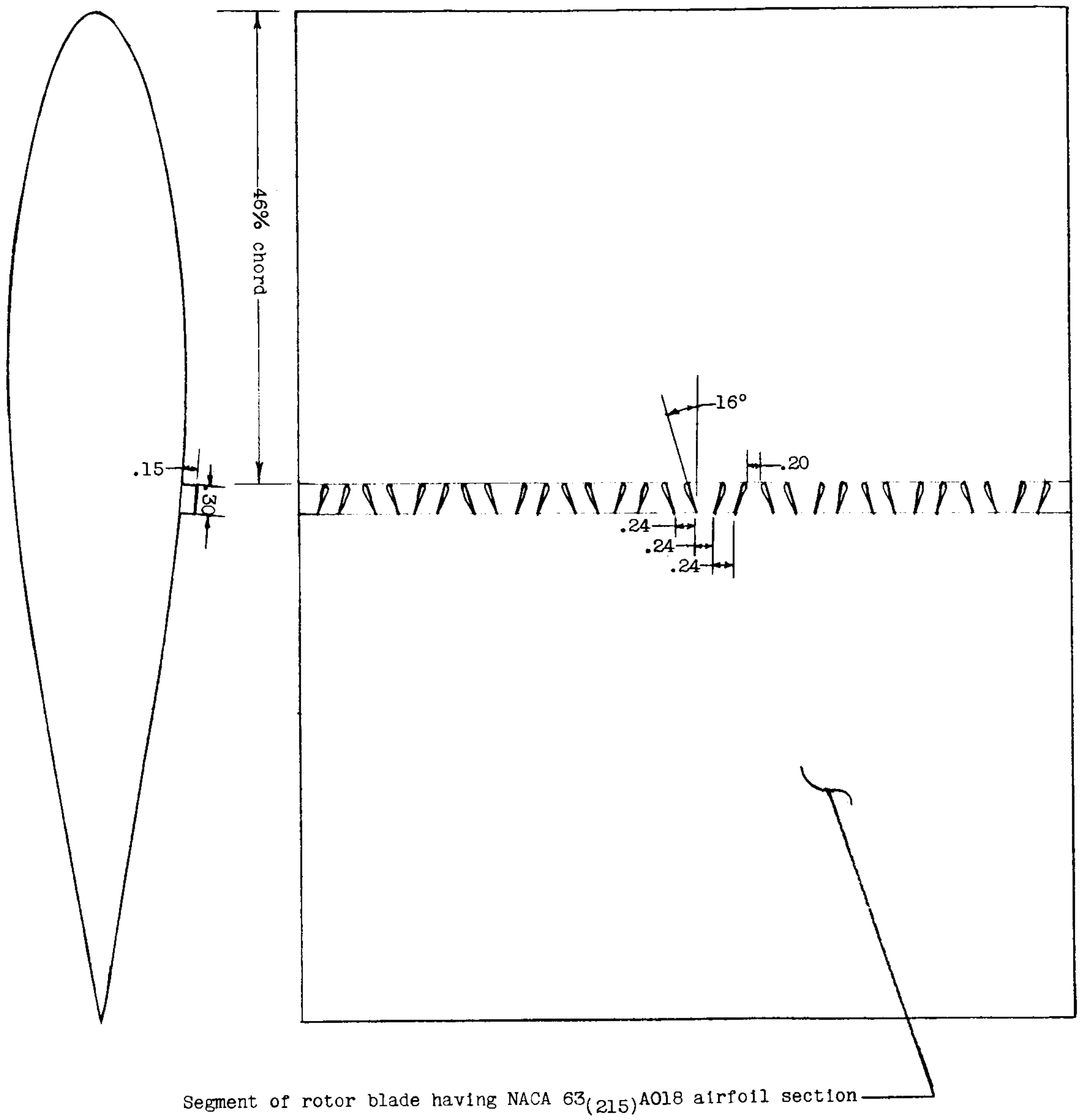

Figure 9.- Vortex-generator installation on rotor blade having NACA $63_{(215)}$A018 airfoil sections. Linear dimensions are in inches.

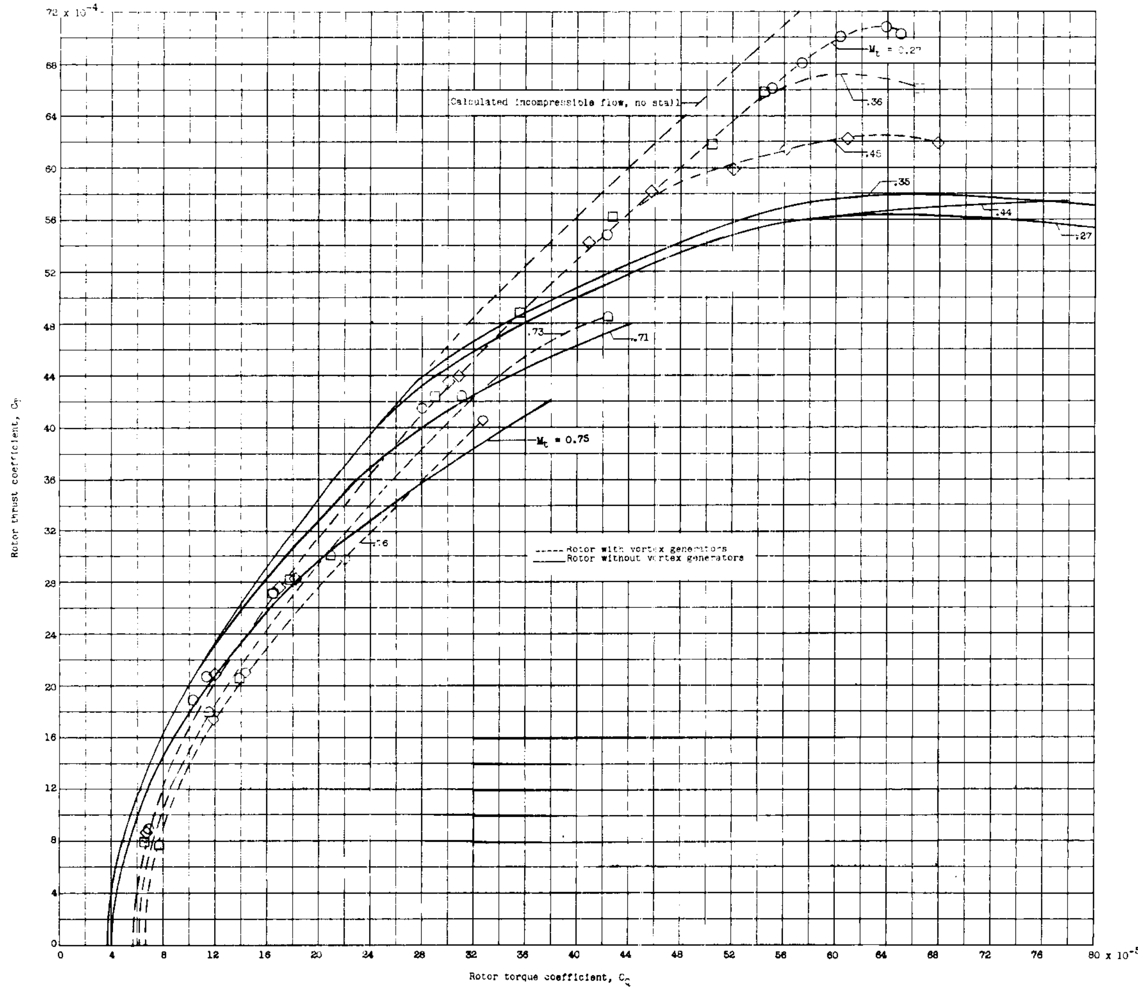

Figure 10.- Comparison of hovering performance for rotor blades having NACA $63_{(215)}$A018 airfoil tip sections with and without vortex generators installed.

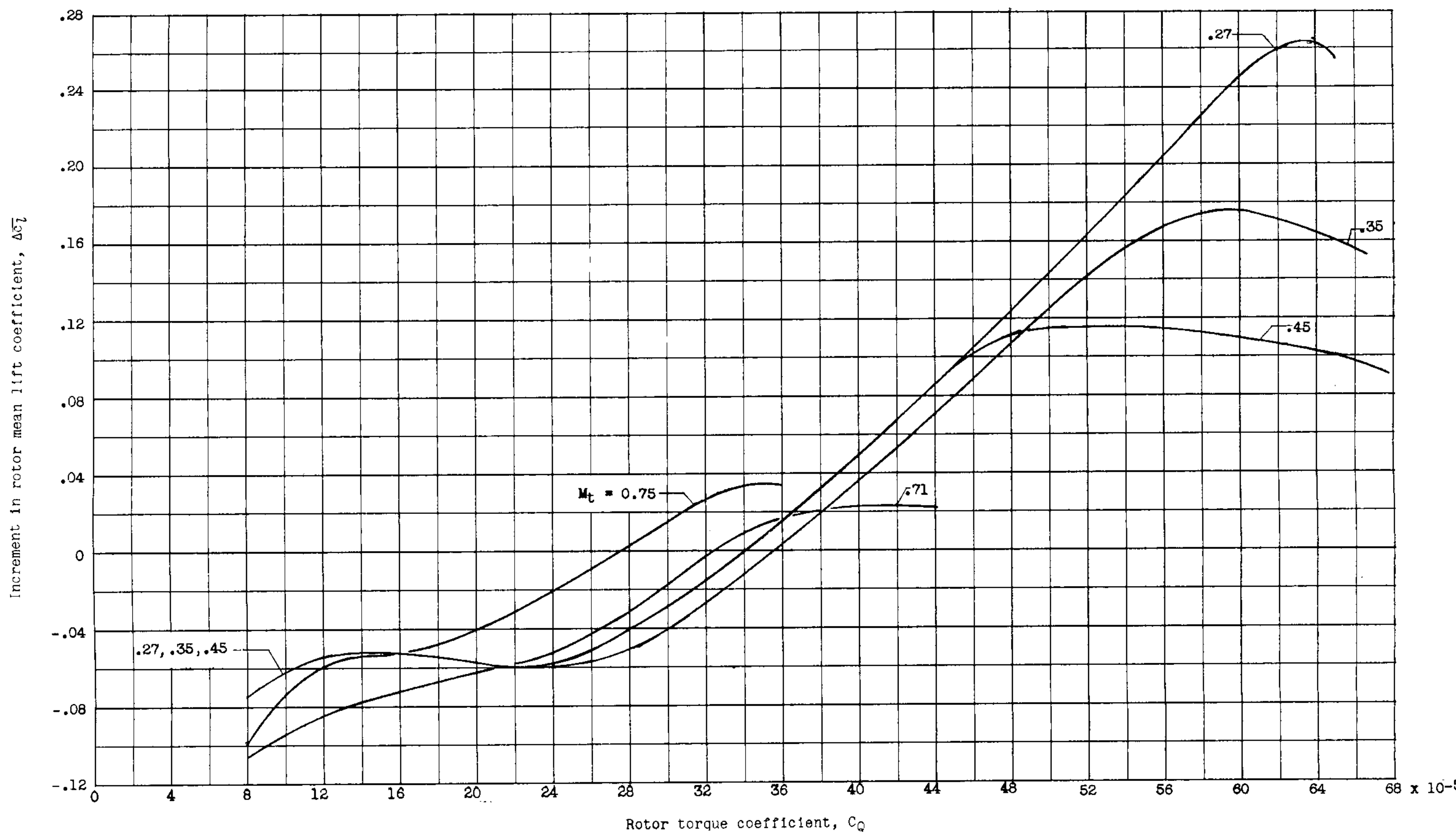

Figure 11.- Gain in rotor mean lift coefficient with the use of vortex generators.

L-311

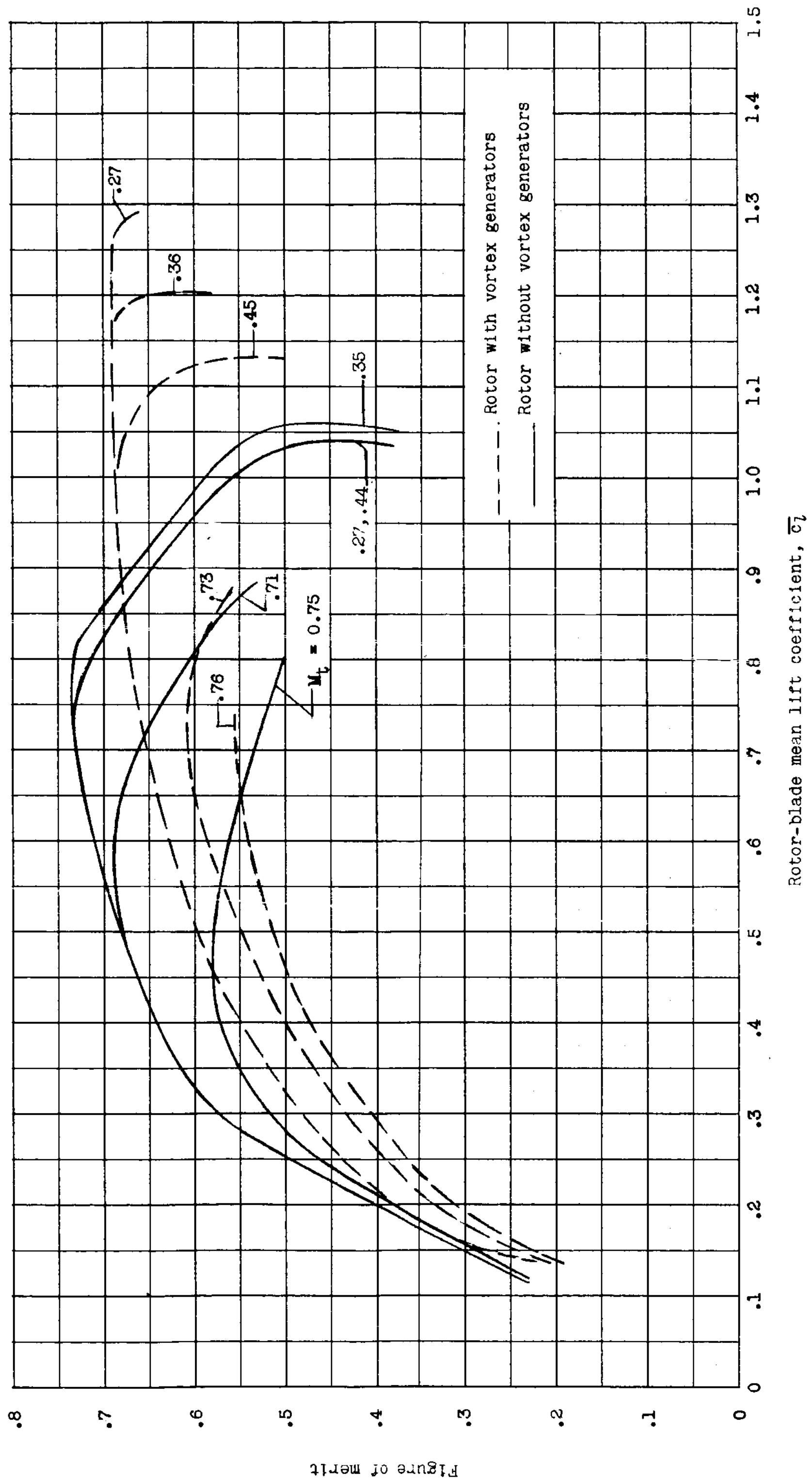

Figure 12.- Comparison of effect of tip Mach number on rotor figure of merit for rotor with and without vortex generators.